Effect of Connection Rigidity on Seismic Response of Precast Concrete Frames

Haluk Sucuoğlu, Ph.D.
Professor of Structural Engineering
Department of Civil Engineering
Middle East Technical University
Ankara, Turkey

Inelastic seismic responses of precast concrete frames and their monolithic counterparts are calculated to evaluate the effect of semi-rigid connections on the seismic behavior of multistory precast frames. Fixity factors defined for precast beam-to-column connections are used as variables in the analytical investigation. It is concluded that the differences between the seismic behaviors of precast and monolithic concrete frames are not significant, provided that the fixity factors remain above 0.80. Strong column-weak beam design plays an important role in reducing these differences. However, it may be necessary to consider the connection rigidity as a design parameter, unless rigid connection behavior is ensured.

An important parameter leading to behavior differences between precast concrete frames and reinforced concrete monolithic frames is the connection rigidity provided at the beam-to-column connections. Monolithic frames possess infinite rigidity at their beam-to-column connections, owing to continuous joint reinforcement details and monolithically cast concrete. It should be noted, however, that monolithic joints may suffer from cracking due to the effects of sustained loads and excessive creep and shrinkage strains, which reduce their rotational connection stiffness from infinite to finite values.

When an end moment M_c is applied to the beam end rigidly connecting to the joint, as shown in Fig. 1(a), the monolithic joint rotates by an amount θ; however, the beam and column axes retain their original relative position and maintain their orthogonality. On the other hand, an additional relative rotation of θ_c occurs between the beam and column axes of the precast frame in a similar condition, displayed in Fig. 1(b), because precast connections possess finite rotational stiffness. The ratio M_c/θ_c is called the rotational connection rigidity.

The semi-rigidity of precast connections is regarded as one of the disadvantages of precast concrete construction compared with cast-in-place construction. This results in the application of more severe measures to the design and construction of precast concrete frames compared to cast-in-place concrete frames, especially in seismic regions. It is possible to provide rigid connections in precast frames by applying post-tensioning to the connection and to the connecting beams.[1,2] However, the focus of this study is on precast frames assembled of precast concrete members with conventional (mild steel) reinforcement details, which are connected by conventional beam-to-column connection techniques.

A beam with semi-rigid connections on both ends can be represented analytically using rotational springs at its ends, as shown in Fig. 2.[3] If the rotational stiffness of the springs or connection rigidity $k_c = M_c/\theta_c$ is known, then the end moment-rotation relationships for the beam with end rotational degrees of freedom θ_i, θ_j can be expressed as:

$$M_i = \frac{EI}{L}\left(k_{ii}\theta_i + k_{ij}\theta_j\right) \quad \text{(1a)}$$

$$M_j = \frac{EI}{L}\left(k_{ji}\theta_i + k_{jj}\theta_j\right) \quad \text{(1b)}$$

where

$$k_{ii} = k_{jj} = \frac{12p}{4-p^2} \quad \text{(2a)}$$

$$k_{ij} = k_{ji} = \frac{6p^2}{4-p^2} \quad \text{(2b)}$$

Here, the parameter p is called the fixity factor and takes values between 0 and 1; 0 for simple hinged connections and 1 for rigid connections. It is expected that the fixity factor for well designed and high quality precast frame connections is close to 1. The relationship between the fixity factor p and the connection rigidity k_c can be obtained through analysis of the beam in Fig. 2 with the aid of Ref. 3:

$$p = \frac{1}{1+\dfrac{3EI}{k_c L}} \quad \text{(3)}$$

The fixed end moments developed at the beam ends under uniformly distributed load q are then modified as:

$$M_{i,j}^{FE} = \left(\pm\frac{6p-3p^2}{4-p^2}\right)\frac{qL^2}{12} \quad \text{(4)}$$

The values for the connection rigidity k_c and, accordingly, the fixity factor p, can only be determined experimentally. In this study, a comparative analytical survey is carried out for possible practical values of the fixity factor p where the inelastic seismic responses of similar precast and cast-in-place concrete frames are calculated and compared to assess the effect of connection rigidity on the seismic frame behavior.

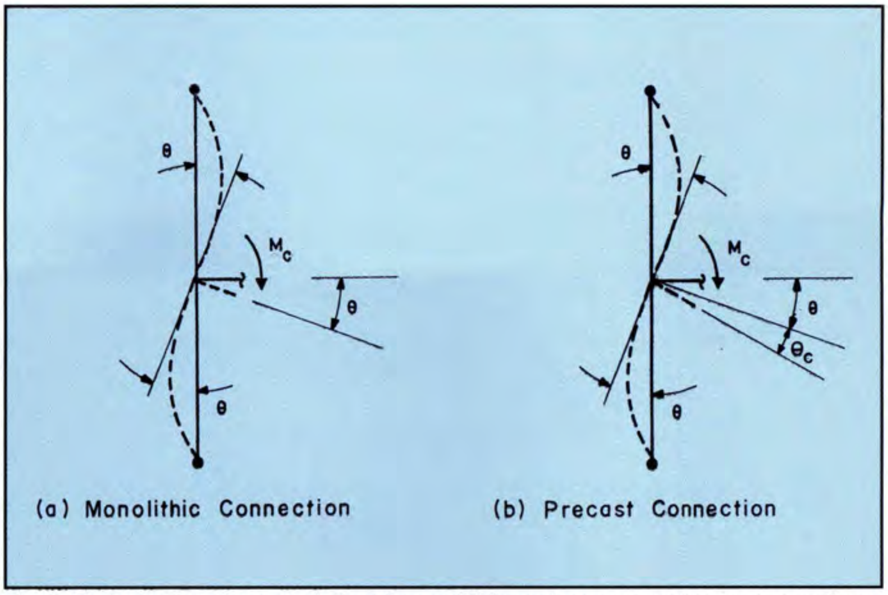

Fig. 1. Deformation characteristics of monolithic and precast concrete connections.

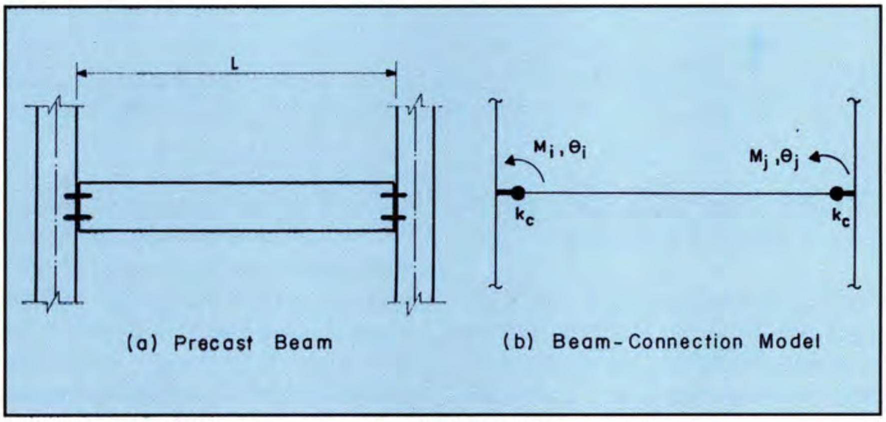

Fig. 2. Modeling of precast connection rigidity using rotational springs.

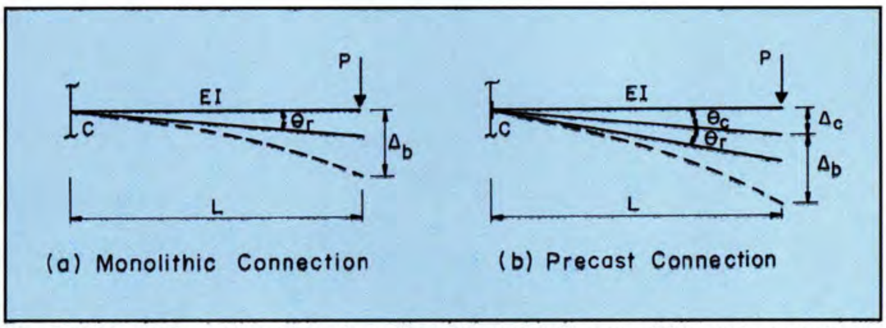

Fig. 3. Deformation properties of cantilever beams with monolithic and precast concrete connections.

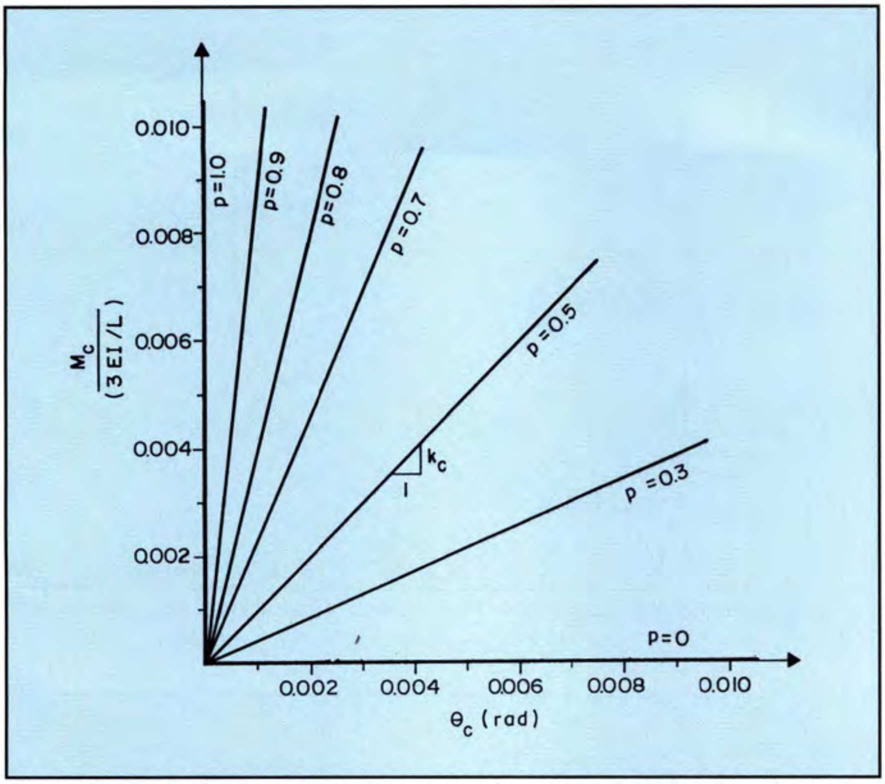

Fig. 4. Linear elastic moment-rotation relationships for semi-rigid connections.

DESCRIPTION OF THE FIXITY FACTOR

The connection rigidity k_c can be determined experimentally by testing companion cantilever beam specimens. The first specimen is cast monolithically with the joint and the second one is a precast beam connected to the joint with a semi-rigid connection. The specimens are schematized in Fig. 3. When a concentrated load P is applied in the elastic range to the free end of the monolithic beam specimen, it causes an end deflection of Δ_b, which is due to both elastic deformations of the beam and rigid body rotation θ_r of the specimen resulting from imperfections in simulating the support conditions.

If the same load is applied to the precast beam specimen, an additional end deflection Δ_c occurs due to connection rotation θ_c, as shown in Fig. 3. This rotation is related to the connection rigidity by:

$$M_{i,j}^{FE} = \left(\pm \frac{6p - 3p^2}{4 - p^2}\right) \frac{qL^2}{12} \quad (5)$$

Hence, the additional deflection of the precast beam is:

$$\Delta_c = \theta_c L_s \quad (6)$$

Substituting θ_c from Eq. (6) into Eq. (5) results in:

$$k_c = \frac{PL_s^2}{\Delta_c} \quad (7)$$

where Δ_c is the difference between the measured total end deflections of a precast and a monolithic cantilever beam with the same length L_s, under the same end load P.

This formulation requires a monolithic specimen, in addition to the precast specimen, to eliminate the contribution of rigid body rotations during testing. If rigid body rotations can be

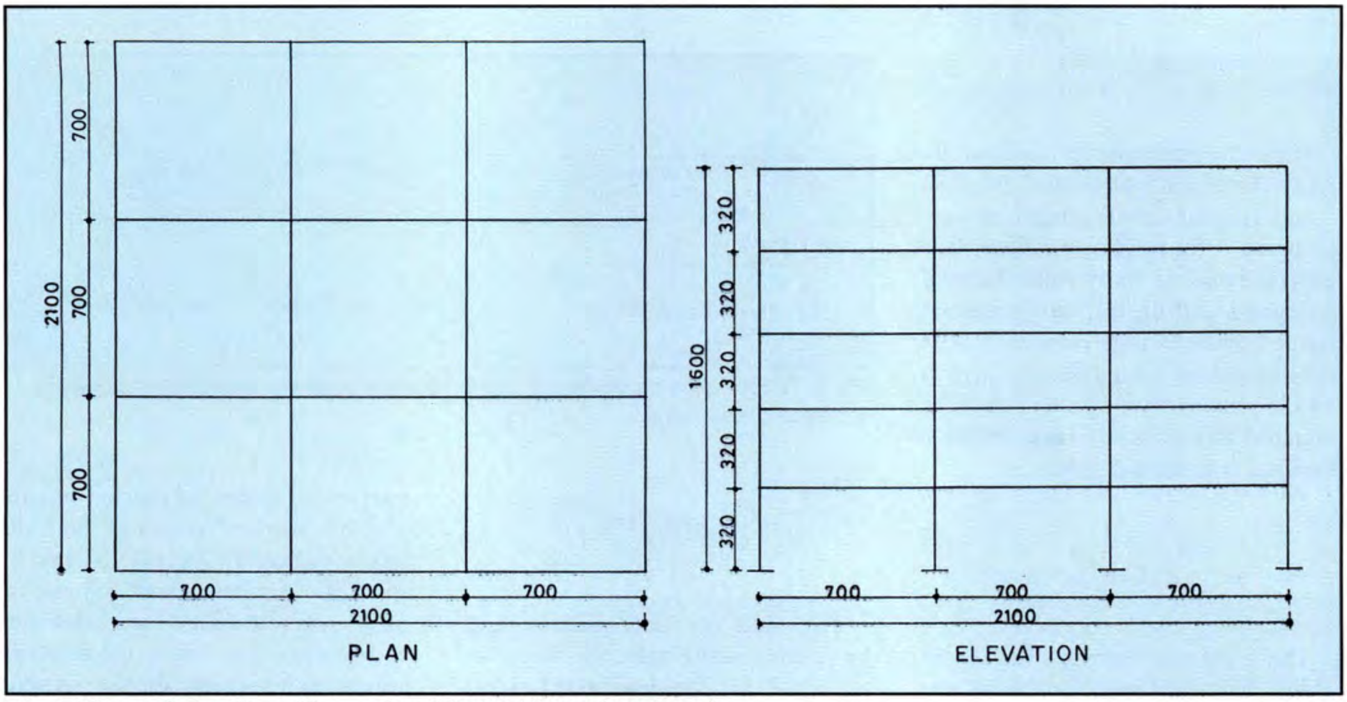

Fig. 5. Plan and elevation of the analyzed frame (dimensions in cm).

Table 1. Flexural capacities of beams (kN-m).

Story	Location	Span		Support	
		M_y^+	M_y^-	M_y^+	M_y^-
1-4	Exterior	209	48	107	348
5	Exterior	169	48	69	239
1-4	Interior	169	48	103	312
5	Interior	136	48	69	239

Note: 1 kN-m = 0.74 kip-ft.

Table 2. Fixity factors and connection rigidities for the analytical models.

Monolithic frame	Precast frame Type I	Precast frame Type II
$p = 1.0$	$p = 0.90$	$p = 0.80$
$k_c = \infty$	k_c = 360,000 kN-m	k_c = 160,000 kN-m

Note: 1 kN-m = 0.74 kip-ft.

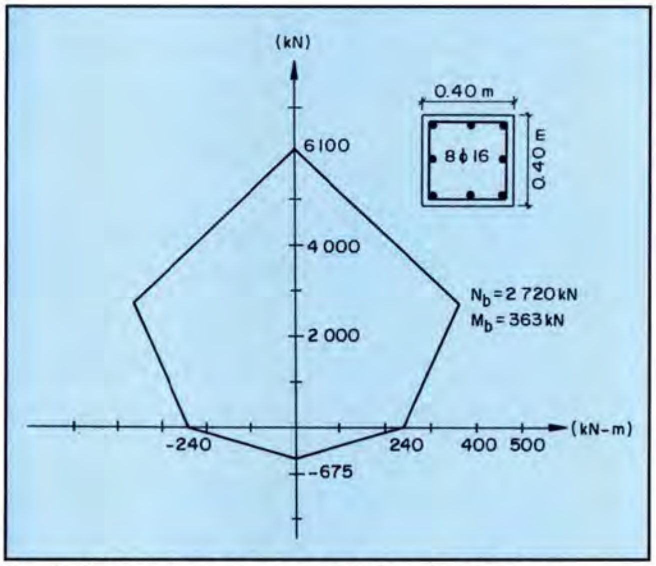

Fig. 6. Column cross section and interaction diagram.

precisely measured and eliminated, then Δ_c can be directly obtained from the precast cantilever specimen because the elastic deformations of the beam itself can be calculated with sufficient accuracy in the linear range.

Once k_c is determined from Eq. (7) for a specific type of precast beam-to-column connection and a beam cross section, it can be used in Eq. (3) to obtain the fixity factor of a precast beam with the same cross section geometry for any length L. The connection moment M_c, rotation θ_c, rigidity k_c, and the fixity factor p can be related to each other with the aid of Eq. (3) and the first part of Eq. (5), and expressed as a family of normalized moment-rotation relationships, as shown in Fig. 4.

There are various experimental studies on precast connections that include the testing of precast and monolithic pairs of cantilever beams. However, because these studies are generally aimed at determining the ultimate connection resistance, their load-deflection behaviors in the initial elastic stage are usually not reported. Refs. 4 to 6 are the available experimental studies that provide information on connection rigidity.

Seckin and Fu[4] obtained identical load-deflection behaviors from their monolithic and precast cantilever pairs at the initial loading stages, owing to the sophisticated details they developed for precast beam-to-column connections. In this extreme case, connection rigidity approaches infinity; thus, the fixity factor becomes 1 in accordance with Eq. (3).

Two pairs of cantilever specimens had been tested at the Middle East Technical University that were manufactured by a precast concrete company.[5,6] The connection rigidities of the precast specimens having cross section dimensions of 0.25 x 0.38 m (10 x 15 in.) had been determined as 38,077 and 43,435 kN-m (28,093 and 32,046 kip-ft) by using the outlined procedure. Considering that beams with the given cross section dimensions can be employed in precast frames having clear span widths of 4 to 5 m (12 to 16 ft), the corresponding fixity factors can be calculated using Eq. (3), which yields values between 0.6 and 0.7.

The above values are relatively low and precast frames employing beams with such low fixity factors should not be considered as rigidly jointed, in view of Fig. 4. Accordingly, the assumption of infinite joint rigidity in the design of precast frames with such beam-to-column connections may lead to unsafe results.

In this study, two fixity factors of 0.80 and 0.90 are implemented in the inelastic dynamic analysis of a precast frame model. The seismic response of the frame is calculated under an earthquake base excitation and the sensitivity of the seismic frame response to the beam fixity factors is evaluated.

ANALYTICAL FRAME MODEL

The dimensions of the precast concrete frame analyzed in this study were chosen to represent a building frame fulfilling the service requirements expected from a precast structure. An internal frame of a typical five-story office building with wide spans was selected for investigation. The frame is shown in Fig. 5. It is assumed that the building has a regular plan geometry with a uniform frame spacing of 7 m (23 ft) in both orthogonal directions and a uniform story height of 3.2 m (10.5 ft).

The frame is designed to conform with the ACI Code provisions.[7] Lateral design loads are specified in accordance with Seismic Zone 4 requirements of the Uniform Building Code,[8] with a response modification factor of 12 assigned for ductile moment resist-

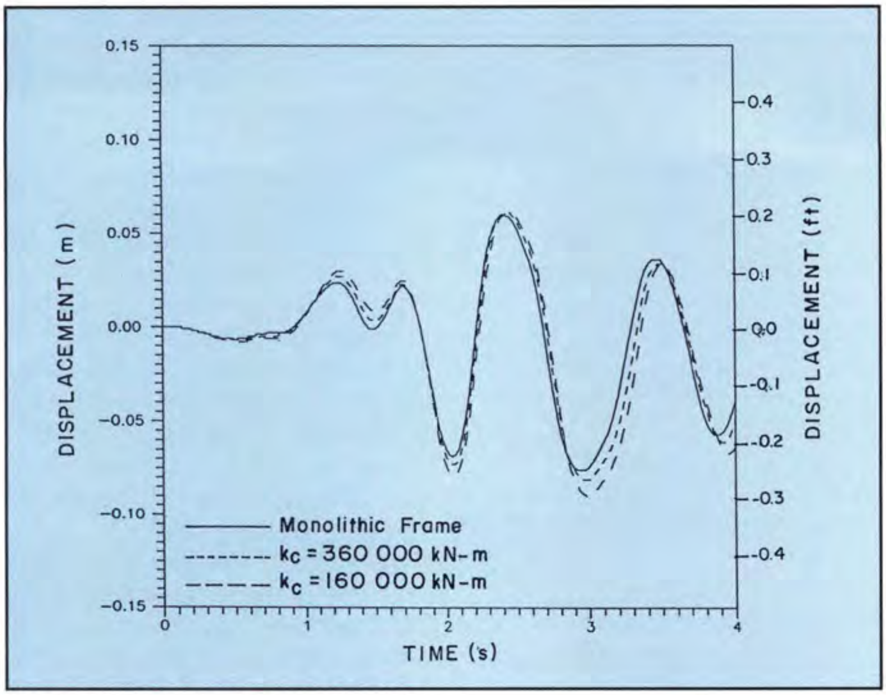

Fig. 7. Fifth story displacement time history.

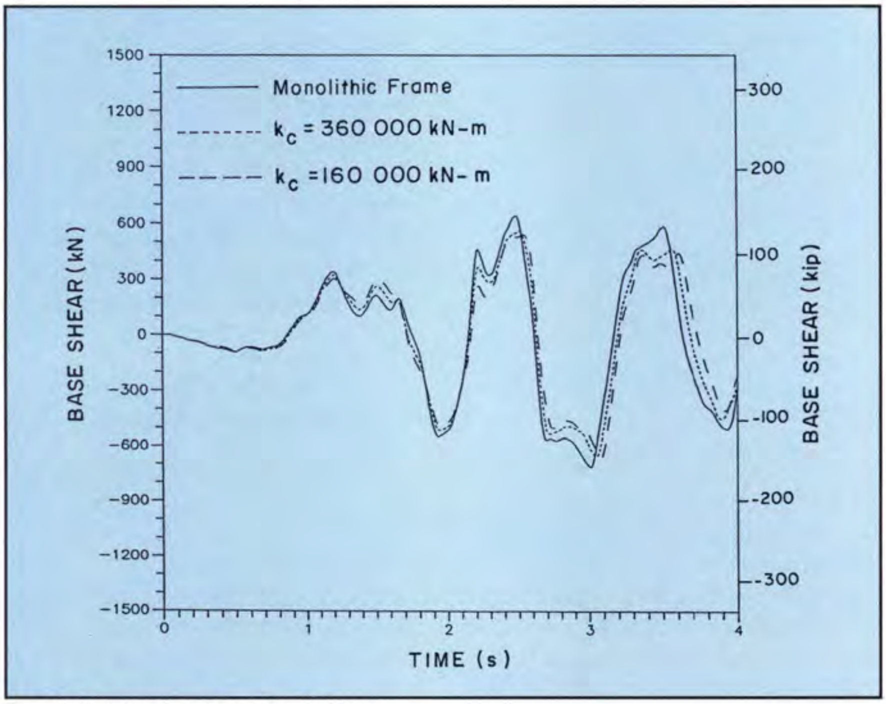

Fig. 8. Total base shear time history.

ing frames. The weight of the frame consists of the self weights of 0.40 x 0.40 m (16 x 16 in.) columns, 0.30 x 0.50 m (12 x 20 in.) beams, 0.16 m (6.3 in.) thick hollow-core slab members, and 0.05 m (2 in.) thick concrete floor cover. In addition, exterior wall panels and interior light partitions, with respective weight intensities of 2.5 and 1 kN/m^2 (0.363 and 0.145 psi), are included in the frame tributary weight. Live load and snow load intensities considered in design are both 2.5 kN/m^2 (0.363 psi).

Material properties are specified as 40 MPa (5800 psi) for the compressive strength of concrete and 420 MPa (61,000 psi) for the yield strength of steel.

All exterior beams, interior beams, and columns are designed for the combination of maximum values of their respective internal forces obtained from the frame analysis, and hence, the cross section properties of the exterior beams, interior beams, and columns are kept constant throughout the frame. Fig. 6 shows the column cross section and its yield interaction diagram.

The column reinforcement required is slightly less than the 1 percent minimum ratio specified for columns in the building codes. The flexural capacities of the beams that are detailed to resist the design forces are given in Table 1. The strong column-weak beam criterion is satisfied at the joints where the ratio of column-to-beam flexural capacities exceeds 6/5.

The connection rigidities calculated for the model frame, using Eq. (3) for the fixity factors of p = 0.80 and p = 0.90, are presented in Table 2. A monolithic frame with similar properties is also included in the analysis for the comparison of dynamic responses.

SEISMIC RESPONSE ANALYSIS AND RESULTS

The precast frame models and their monolithic counterpart are analyzed under the El Centro 1940 NS ground excitation using the DRAIN-2D program.[9] One beam/column element with elasto-plastic hysteresis model is used for each column member, whereas three beam elements with the degrading stiffness hysteresis model are employed to represent each beam. A strain hardening ratio of 5 percent is accepted for all hysteresis models and 5 percent damping is assumed for all elements. Integration of the equations of motion is carried out at constant time steps of 0.005 seconds. Response duration is limited to 4 seconds because the maximum responses occur between 2.5 and 3 seconds. Gravity loads are applied on the frames prior to dynamic analysis.

Semi-rigid precast connections lead to reductions in the beam stiffnesses and, consequently, reduction in the lateral stiffness of precast frames with reference to the monolithic frames. The effects of these variations on the global frame response and the local responses of precast beams are presented and discussed separately in the following sections.

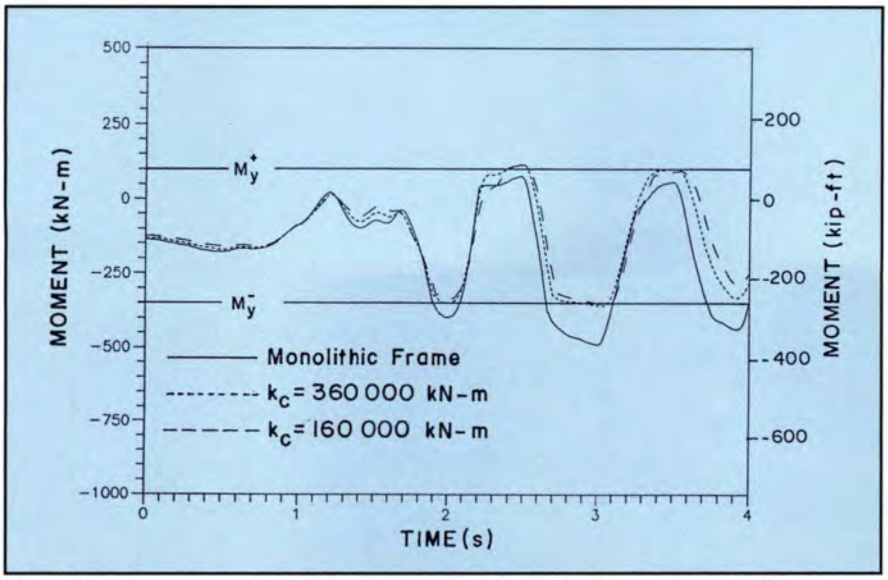

Fig. 9. Bending moment time history at left end of first story left exterior beam.

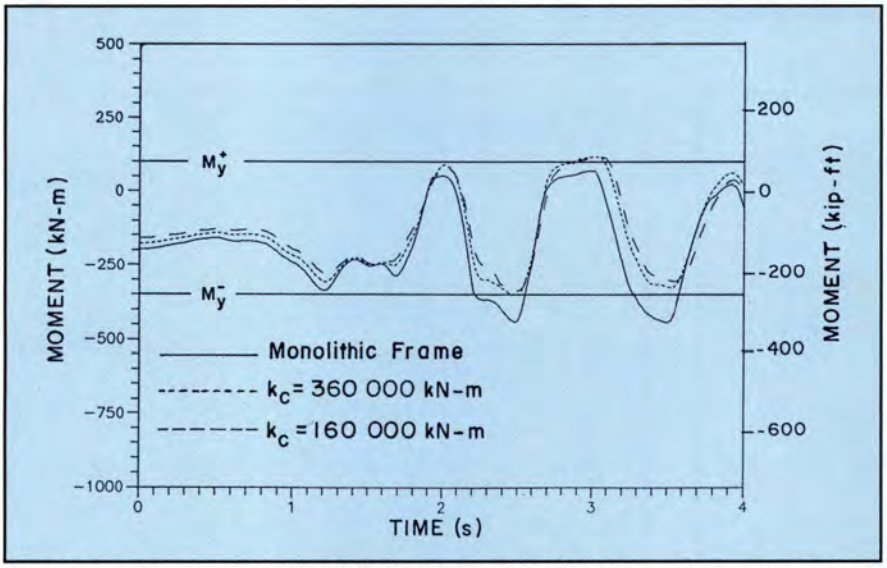

Fig. 10. Bending moment time history at right end of first story right exterior beam.

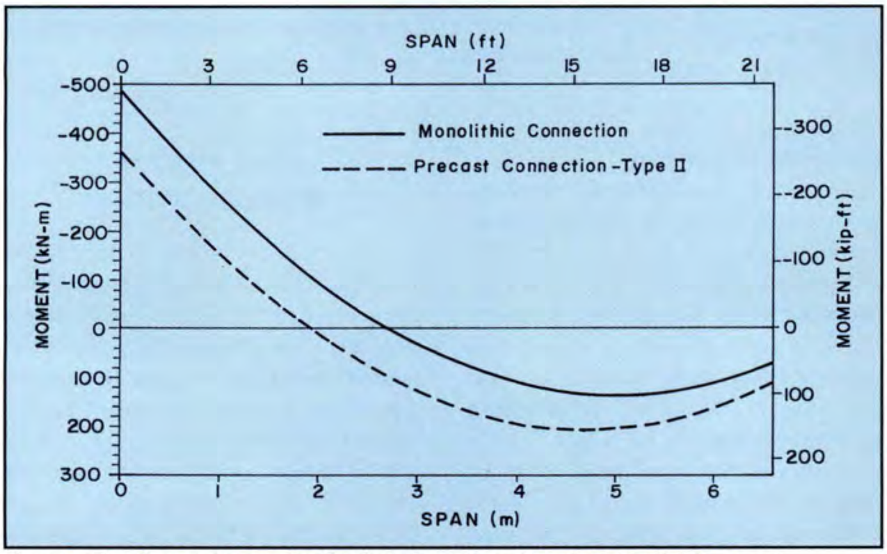

Fig. 11. Bending moment distribution along first story left exterior beam at $t = 3$ seconds (positive moment creates tension at bottom fibers).

Lateral Frame Stiffness

The first mode vibration period of the monolithic frame is 0.945 seconds, whereas that of the precast frame with Type II connections is 1.052 seconds. Hence, the initial lateral elastic stiffness of the Type II precast frame is 24 percent less than the initial stiffness of the monolithic frame. Story displacements increase and base shear forces decrease in the precast frames, with respect to the monolithic frame, as a consequence of their reduced initial stiffnesses; however, these changes are not very significant.

The time history of the fifth story displacements and the total base shear forces under the El Centro ground excitation are shown in Figs. 7 and 8. Fifth story maximum lateral displacement of the Type II precast frame increases by 20 percent and its maximum total base shear force decreases by 10 percent. When it is considered that the sequences of plastic hinge formation in the columns of precast and monolithic frames are very similar, these differences in the lateral frame responses can be simply attributed to the differences in their initial elastic lateral stiffnesses.

Bending Moment Distribution in Beams

Decreasing connection rigidity has a different effect on the beam moment distribution. Bending moment magnitudes along the beam axis shift in a direction where negative moments decrease and positive moments increase as the connection rigidities decrease.

The left and right end bending moment time histories of the first story left exterior beam are presented in Figs. 9 and 10. Under the gravity loads applied to all three frames prior to dynamic analysis, beam end moments decrease by 10 and 20 percent, respectively, in Types I and II precast frames with respect to the monolithic frame. These variations can be observed in Figs. 9 and 10 at $t = 0$ second. Positive beam span moments increase at similar ratios under gravity loads.

The variations in the beam bending moment distributions under earthquake excitation are different due to reversals in its direction. Figs. 9 and

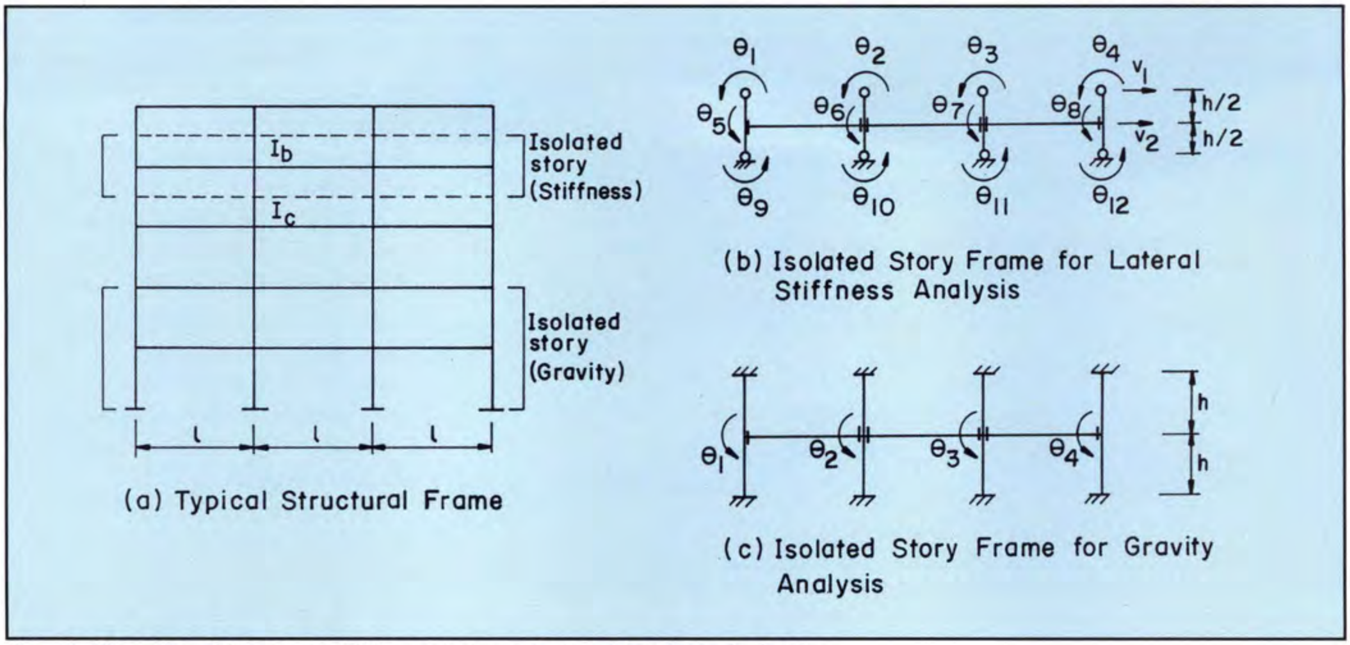

Fig. 12. Elements of frame sensitivity analysis under lateral and gravity loads.

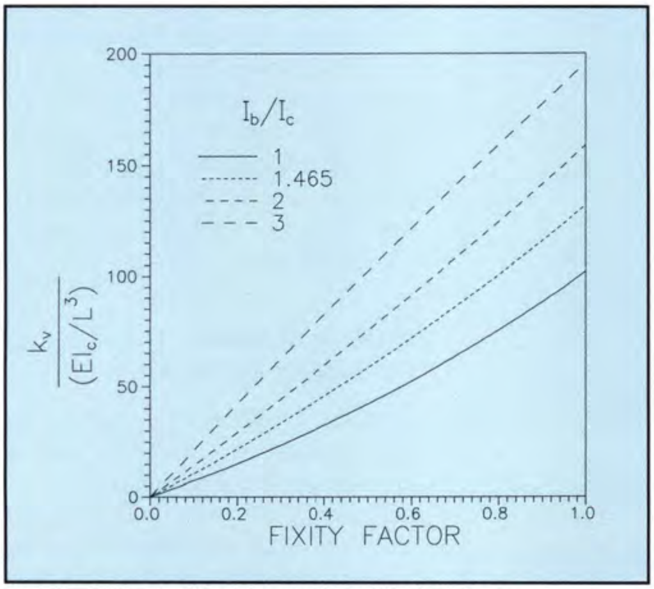

Fig. 13. Lateral stiffness variation with fixity factor.

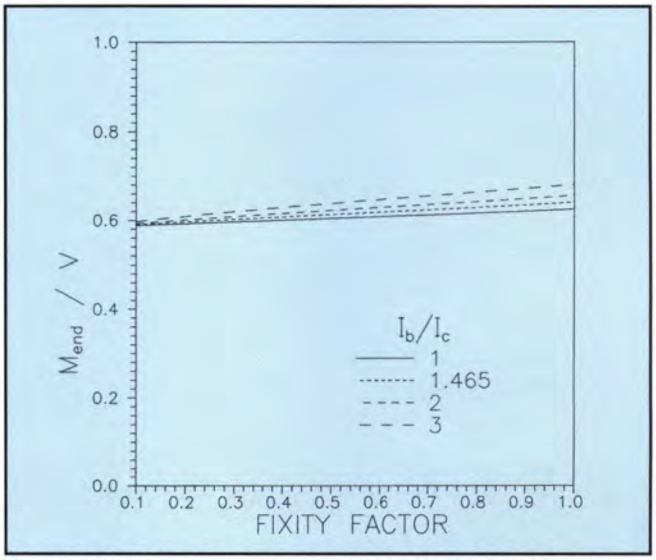

Fig. 14. Variation of beam end moments with fixity factor under lateral forces.

10 indicate that the beam ends of the monolithic frame only yield in the negative direction, whereas positive yielding occurs in precast beams as their connection rigidities decrease. However, the differences between the end moments of the two types of precast beams disappear when their ends yield because plastic hinge rotations overcome connection rotations at the beam ends after yielding begins. Therefore, the inelastic seismic behavior of precast beams with semi-rigid connections should be considered different from the behavior of their monolithic counterparts.

The bending moment distributions along the first story left exterior beam in monolithic and Type II precast frames are compared in Fig. 11 at $t = 3$ seconds, when the response is maximum. Positive support and span moments increase significantly in the precast beam in exchange for reduction in the negative support moments. Thus, a ground excitation equivalent to El Centro 1940 may develop plastic hinges on the span of the precast beam if fixity factors of semi-rigid connections fall below 0.80.

ANALYTICAL VERIFICATION

The sensitivity of lateral frame stiffness and beam bending moments of a typical precast frame to the beam-to-column connection rigidity can be assessed by analyzing a story frame isolated from the entire frame. A typical frame structure is shown in Fig. 12(a). The inflection points on the columns at an intermediate story develop at approximately the mid-height under lateral loads. Hence, the isolated frame shown in Fig. 12(b) can be employed

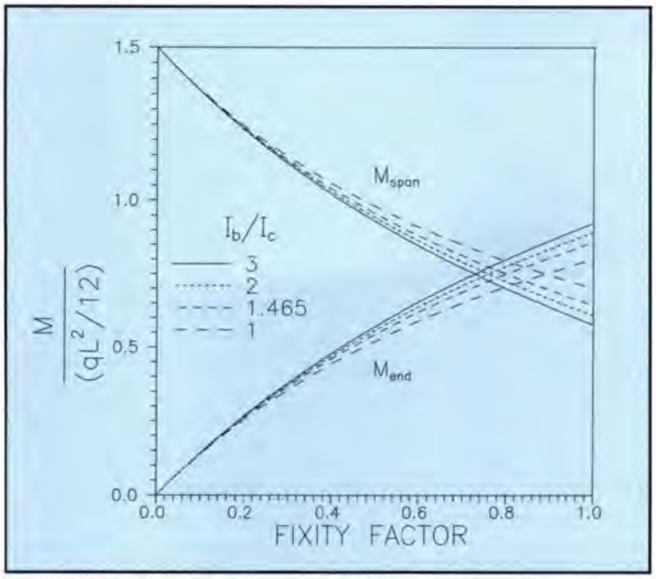

Fig. 15. Variations of beam end moments and midspan moments with fixity factor under uniform span loading.

to define the story lateral stiffness.

If infinite axial stiffness is assumed for columns and beams, and symmetry of the isolated frame is taken into consideration, the degrees of freedom of the isolated story decrease from 14 to 6. The 6 x 6 stiffness matrix presented in Appendix A includes the fixity factor p in accordance with Eqs. (1) and (2). A story lateral stiffness can be calculated in terms of the member properties and the fixity factor by condensing the stiffness matrix into the relative story displacement degree of freedom v_1, as presented in Appendix A.

The calculated story stiffness is plotted in Fig. 13 as a function of the fixity factor p for various beam-to-column cross section inertia ratios in which 1.465 is the ratio for the frame analyzed in the previous section. It can be observed that the story stiffness is almost linearly related to the fixity factor and the stiffness reduction at $p = 0.80$ is 25 percent, which matches the reduction calculated for the Type II frame with respect to the monolithic frame.

The same story frame model is used for calculating the beam end moments developed under the applied story shear forces (see Appendix A). Fig. 14 presents the results where the beam end moments display almost no sensitivity to the fixity factor. Although the end rotations increase in proportion to the decrease in the fixity factor, this is not reflected in the beam end moments because of a simultaneous reduction in the beam rotational stiffness, as indicated in Eq. (A7).

The variation of the beam support and span moments with the fixity factor is also calculated under uniform span load q by employing a slightly different isolated story frame, as indicated in Fig. 12(a) and shown in detail in Fig. 12(c). The analytical evaluation is given in Appendix A and the results are presented in Fig. 15. A strong interaction between the beam moments and the fixity factor is apparent under gravity loads, in contrast to the lateral loads.

These results indicate different influences of semi-rigid connections on frame behavior at global and local levels. Lateral stiffness of the precast frames decreases against seismic loads, which has no consequence on the beam moments. On the other hand, moment distributions in beams under gravity loads are significantly affected by the variations in connection rigidity.

A parametric analytical evaluation using isolated portions of the structural frame has proven to be very effective in predicting the variations in frame lateral stiffness and beam bending moments in the linear elastic range due to the semi-rigidity of connections. Considering that structural design is essentially based on linear elastic analysis, such an approach may be followed for modifying the design forces to account for the finite connection rigidity in precast frames.

CONCLUSIONS

Based on this study, the following conclusions are derived:

1. Precast concrete frames have reduced lateral stiffnesses due to the effect of semi-rigid beam-to-column connections. However, if the connections are well designed and are of high quality, such that the beam fixity factors are above 0.80, the seismic responses of the precast frames are not significantly different from their monolithic counterparts.

2. The strong column-weak beam concept in seismic design of precast frames is very effective in compensating for the unfavorable effects of semi-rigid connections on the seismic response of precast frames.

3. Reduction in connection rigidity leads to an overall shift in the beam bending moment distribution along the beam span from negative to positive moment magnitudes under combined seismic and gravity loads.

4. Beam moments are not very sensitive to the rigidity of connections under lateral loads applied on the frame; however, they are sensitive to connection rigidity under gravity loads distributed over the beam span.

5. The connection rigidity can be considered as a design parameter unless sufficient rigidity is ensured for the precast connections employed in construction.

6. Simple isolated story frame models may be used to assess the influence of semi-rigid beam-to-column connections on the precast frame response and, accordingly, for modifying the design forces.

ACKNOWLEDGMENT

The research presented in this paper was supported by the Turkish Scientific and Technical Research Council and the Turkish Precast Association under Grant No. MAG 739/A. This support is gratefully acknowledged. The assistance provided by graduate students Ali Y. Kus and Bülent Alemdar is greatly appreciated.

REFERENCES

1. Cheok, Geraldine S., and Lew, H. S., "Performance of Precast Concrete Beam-to-Column Connections Subject to Cyclic Loading," PCI JOURNAL, V. 36, No. 3, May-June 1991, pp. 56-67.
2. French, C. W., Haffner, M., and Jayashankar, V., "Connections Between Precast Elements — Failure Within Connection Region," *ASCE Journal of Structural Engineering*, V. 115, No. 12, 1989, pp. 3171-3192.
3. Wang, C. K., *Intermediate Structural Analysis*, Chapter 20, McGraw-Hill, 1983.
4. Seçkin, M., and Fu, H. C., "Beam-Column Connections in Precast Reinforced Concrete Construction," *ACI Structural Journal*, V. 87, No. 3, 1990, pp. 252-261.
5. Baysal, M. Z., "Behavior of an Exterior Precast Beam-Column Connection Under Reversed Cyclic Loading," M.S. Thesis, Department of Civil Engineering, Middle East Technical University, Ankara, Turkey, 1991.
6. Yagci, S., "Behavior of an Improved Exterior Precast Beam-Column Connection Under Reversed Cyclic Loading," M.S. Thesis, Department of Civil Engineering, Middle East Technical University, Ankara, Turkey, 1993.
7. ACI Committee 318, "Building Code Requirements for Reinforced Concrete (ACI-318-89)," American Concrete Institute, Detroit, MI, 1989.
8. *Uniform Building Code* (UBC-91), International Conference of Building Officials, Whittier, CA, 1991.
9. Kanaan, A. E., and Powell, G. H., "DRAIN-2D: A General Purpose Computer Program for Dynamic Analysis of Inelastic Plane Structures," Earthquake Engineering Research Center, EERC 73-6, 73-22, University of California, Berkeley, CA, 1973.
10. Wolfram, S., *Mathematica: A System for Doing Mathematics by Computer*, Addison-Wesley Publishing Co., Redwood City, CA, 1988.

APPENDIX A — STRUCTURAL PROPERTIES OF AN ISOLATED STORY FRAME WITH SEMI-RIGID BEAM-TO-COLUMN CONNECTIONS

The stiffness matrix of a beam element with semi-rigid end connections that has the degrees of freedom indicated in Fig. A1 is:

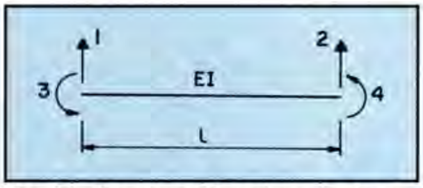

Fig. A1. Degrees of freedom of a beam element.

$$\underline{k} = \frac{EI}{l^3}\begin{bmatrix} 12 & -12 & 6l & 6l \\ -12 & 12 & -6l & -6l \\ 6l & -6l & k_{ii}l^2 & k_{ij}l^2 \\ 6l & -6l & k_{ji}l^2 & k_{jj}l^2 \end{bmatrix} \tag{A1}$$

where k_{ii}, k_{jj}, k_{ij} and k_{ji} are defined in Eqs. (2a) and (2b).

The stiffness matrix of the isolated story frame shown in Fig. 12(b) can be obtained by assembling the element stiffness matrices of beams and columns. If the axial deformations of the frame members are ignored and the lateral displacements of columns are assumed equal due to the axial rigidity of floor beams and diaphragms, the degrees of freedom reduce to 14, as indicated in Fig. 12(b). Further, when the constraint conditions $\theta_1 = \theta_4 = \theta_9 = \theta_{12}$; $\theta_2 = \theta_3 = \theta_{10} = \theta_{11}$; $\theta_5 = \theta_8$ and $\theta_6 = \theta_7$ are imposed due to the symmetry of the isolated frame, the degrees of freedom reduce to 6. The stiffness matrix calculated accordingly, by assuming $h = l/2$, is obtained as:

$$\underline{K} = \frac{2EI_c}{l^3}\begin{bmatrix} 1536 & -1536 & 96l & 96l & 96l & 96l \\ & 3072 & 0 & 0 & 0 & 0 \\ & & 32l^2 & 0 & 16l^2 & 0 \\ & SYM. & & 32l^2 & 0 & 16l^2 \\ & & & & a & b \\ & & & & & (b+c) \end{bmatrix} \tag{A2}$$

where

$$a = 32l^2 + 12l^2\frac{I_b}{I_c}\frac{p}{\left(4-p^2\right)} \tag{A3}$$

$$b = 6l^2\frac{I_b}{I_c}\frac{p^2}{\left(4-p^2\right)} \tag{A4}$$

$$c = 32l^2 + 24l^2\frac{I_b}{I_c}\frac{p}{\left(4-p^2\right)} \tag{A5}$$

and the remaining degrees of freedom are ordered such that the displacement vector becomes $\underline{U}^T = \{v_1, v_2, \theta_1, \theta_2, \theta_5, \theta_6\}$. A lateral story stiffness expression k_v can be obtained by statically condensing the last five degrees of freedom into the first degree of freedom v_1.

$$k_v = \frac{2EI_c}{l^3}\left[\underline{k}_{11} - \underline{k}_{1r}^T\underline{k}_{rr}^{-1}\underline{k}_{1r}\right] \tag{A6}$$

Here, k_{11}=1536, $\underline{k}_{1r}$ is the first column of the stiffness matrix in Eq. (9) except the first element, and $\underline{k}_{rr}$ is the lower right 5 x 5 portion of the stiffness matrix. Eq. (13) is evaluated parametrically using *Mathematica*.[10] The results shown in Fig. 13 are presented for l = 7 m (275.6 in.) because the elements of the stiffness matrix in Eq. (9) are not dimensionally equivalent.

When a horizontal force V is applied along v_1, the displacement vector $\underline{U}$ can be calculated by solving the linear system $\underline{K}\underline{U} = \underline{P}_v$, where $\underline{P}_v = \{V, 0, 0, 0, 0, 0\}_T$. Then the end moments for the left exterior beam are obtained from:

$$\begin{bmatrix} M_5 \\ M_6 \end{bmatrix} = \frac{EI_b}{l} \begin{bmatrix} k_{ii} & k_{ij} \\ k_{ji} & k_{jj} \end{bmatrix} \begin{bmatrix} \theta_5 \\ \theta_6 \end{bmatrix} \tag{A7}$$

The variation of M_5 with the fixity factor p for various I_b/I_c ratios are shown in Fig. 14.

A gravity load analysis under uniform load q is carried out by isolating a slightly different story frame, shown in Fig. 12(c). The matrix equations of equilibrium for this frame are obtained as:

$$\frac{EI_c}{l} \begin{bmatrix} d & e & 0 & 0 \\ & f & e & 0 \\ SYM. & & f & e \\ & & & d \end{bmatrix} \begin{bmatrix} \theta_1 \\ \theta_2 \\ \theta_3 \\ \theta_4 \end{bmatrix} = \begin{bmatrix} -M^{FE} \\ 0 \\ 0 \\ M^{FE} \end{bmatrix} \tag{A8}$$

in which:

$$d = 16 + 12 \frac{I_b}{I_c} \frac{p}{\left(4 - p^2\right)} \tag{A9}$$

$$e = 6 \frac{I_b}{I_c} \frac{p^2}{\left(4 - p^2\right)} \tag{A10}$$

$$f = 16 + 24 \frac{I_b}{I_c} \frac{p}{\left(4 - p^2\right)} \tag{A11}$$

$$M^{FE} = \frac{ql^2}{12} \frac{\left(6p - 3p^2\right)}{\left(4 - p^2\right)} \tag{A12}$$

The end moments of the left exterior beam are in turn calculated from:

$$\begin{bmatrix} M_1 \\ M_2 \end{bmatrix}_{end} = \begin{bmatrix} M^{FE} \\ M^{FE} \end{bmatrix} + \frac{EI_b}{l} \begin{bmatrix} k_{ii} & k_{ij} \\ k_{ji} & k_{jj} \end{bmatrix} \begin{bmatrix} \theta_1 \\ \theta_2 \end{bmatrix} \tag{A13}$$

where θ_1 and θ_2 are obtained from the solution of Eq. (A8) and the elements of the beam rotational stiffness matrix are defined in Eqs. (1a), (1b), (2a), and (2b). Accordingly, the bending moment at the midspan of the exterior beam is:

$$M_{span} = \frac{ql^2}{8} - \frac{\left(M_1 + M_2\right)_{end}}{2} \tag{A14}$$

The exterior end moment and span moment of the left bay beam obtained by solving Eqs. (A8) to (A14) are presented in Fig. 15 for various I_b/I_c ratios in normalized, dimensionless form. These results are valid for any span length l and uniform load intensity q.

APPENDIX B — NOTATION

E = modulus of elasticity
I_b = moment of inertia of beam
I_c = moment of inertia of column
k = member of the element stiffness matrix
k_v = lateral story stiffness
L, l = beam span length
M_c = connection moment
M_{end} = end moment
M^{FE} = fixed end moment
M_i = bending moment at left end of beam
M_j = bending moment at right end of beam
M_{span} = span moment
M_y = yield moment
P = concentrated force
p = fixity factor
q = uniform load intensity
V = shear force
v = lateral joint displacement
Δ = tip deflection of a cantilever beam
θ = joint rotation
θ_c = connection rotation
θ_i = rotation at left end of beam
θ_j = rotation at right end of beam
$\underline{K}$ = structural stiffness matrix
$\underline{U}$ = displacement vector
$\underline{P}_v$, = load vector
$\underline{k}$ = element stiffness matrix
$\underline{k}_{1r}$, $\underline{k}_{rr}$ = partitions of stiffness matrix